



**PHYSICOCHEMICAL CHANGES OF CORN STARCH DURING LACTIC ACID  
FERMENTATION WITH *Lactobacillus bulgaricus***

**CAMBIOS FÍSICOQUÍMICOS DE ALMIDÓN DE MAÍZ DURANTE LA  
FERMENTACIÓN ÁCIDO LÁCTICA CON *Lactobacillus bulgaricus***

I. Reyes<sup>1</sup>, C. Hernández-Jaimes<sup>1\*</sup>, M. Meraz<sup>2</sup>, M.E. Rodríguez-Huezo<sup>3</sup>

<sup>1</sup>*Facultad de Ciencias. Universidad Autónoma del Estado de México. Campus el cerrillo, Toluca, Estado de México, 50000. México.*

<sup>2</sup>*Departamento de Biotecnología. Universidad Autónoma Metropolitana-Iztapalapa. Apartado postal 55-534. Iztapalapa, Ciudad de México, 09340. México.*

<sup>3</sup>*Departamento de Ingeniería Química y Bioquímica. Tecnológico de Estudios Superiores de Ecatepec, Av. Tecnológico s/n esq. Av. Central, Col. Valle de Anáhuac, Ecatepec, Estado de México, 55210. México.*

Received September 2, 2017; Accepted October 24, 2017

**Abstract**

Lactic acid fermentation (LAF) has been used since antiquity to conserve food including starchy food. The bioaccessibility of starch depends on the food microstructures. Therefore, the understanding of the physicochemical transformations of the starch suffered during LAF will allow to develop an adequate processing of the alimentary matrices. In this work, native corn starch (NCS) dispersions were inoculated with *Lactobacillus bulgaricus* ( $2 \times 10^7$  cells ml<sup>-1</sup>) and fermented for 24 h at 38 °C.

Physicochemical changes of starch granules during fermentation time were monitored by XRD, FTIR and DSC. The crystallinity content achieved a maximum value (39.72±1.02%) after 12 h of fermentation. In contrast, the absorbance ratio 1047/1022 from FTIR measurements increased as the fermentation advanced. Likewise, DSC analysis showed that the gelatinization enthalpy increased 60.0% after 12 h of fermentation, reflecting the production of ordered microstructures. Thus, it is suggested that LAF increased the resistant starch content in corn starch granules.

**Keywords:** corn starch, lactic acid fermentation, *Lactobacillus bulgaricus*, structural changes, cristallinity.

**Resumen**

La fermentación ácido láctica (FAL) ha sido usada desde la antigüedad para conservar diferentes tipos de alimentos incluyendo aquellos que contienen almidón. La bioaccesibilidad del almidón depende de la microestructura del alimento. Por lo tanto, el conocimiento de las transformaciones físicoquímicas que sufre el almidón durante la fermentación ácido láctica permitirá el desarrollo del adecuado procesamiento de las matrices alimenticias. En este trabajo, dispersiones del almidón de maíz nativo (AMN) fueron inoculadas con *Lactobacillus bulgaricus* ( $2 \times 10^7$  células ml<sup>-1</sup>) y fermentadas por 24 h a 38 °C. Los cambios físicoquímicos de los gránulos de almidón durante el tiempo de fermentación fueron monitoreados por DRX, FTIR y DSC. Los resultados mostraron que el contenido de cristalinidad alcanzó un valor máximo (39.72±1.02%) después de 12 h de fermentación. En contraste, la proporción de absorbancia 1047/1022 de las mediciones de FTIR incrementó a medida que avanzó la fermentación. De igual manera, los análisis de DSC mostraron que la entalpía de gelatinización incrementó 60.0% después de 12 h de fermentación, reflejando la producción de microestructuras ordenadas. Así, esto sugiere que FAL incrementó el contenido de almidón resistente en los gránulos del almidón de maíz.

**Palabras clave:** almidón de maíz, fermentación ácido láctica, *Lactobacillus bulgaricus*, cambios estructurales, cristalinidad.

**1 Introduction**

Lactic acid fermentation (LAF) is nowadays one of the most important processes in the food industry. Its attractiveness relies on the wide diversity of natural

and engineered lactic acid consortiums, as well as to the easiness of the operation of the underlying process. Besides, most lactic acid bacteria are tagged as generally recognized as safe (GRAS) medium by the Food and Drug Administration (FDA). LAF is involved in the processing and preservation of dairy

\* Corresponding author. E-mail: carmenhernandezjaimes@gmail.com

Tel/Fax. 72-22-96-55-56.

doi: 10.24275/uam/izt/dcbi/revmexingquim/2018v17n1/Reyes

issn-e: 2395-8472

products, vegetables and fruits, as well as in the bread production via sourdough fermentation (Leroy *et al.*, 2004).

The list of applications and uses of lactic acid bacteria is wide and diverse. Fermented milk products with enhanced functional properties with potential benefits to human health have been traditionally produced by LAF (Shiby and Mishra, 2013). Recently, Di Cagno *et al.* (2013) pointed out that LAF represents the easiest and the most suitable way for increasing the daily consumption of fresh-like vegetables and fruits. The main idea is to combine ancient methods of bio-preservation with novel biotechnology knowledge in order to enhance the safety, nutritional, sensory and shelf life properties of vegetables and fruits. LAF is also used for the large-scale production of lactic acid, which is considered as a commodity for manufacturing derivatives in food, chemical, cosmetic, and pharmaceutical industries (Datta and Henry 2006; Abdel-Rahman *et al.*, 2013). Lactic acid bacteria are used to preserve edible food materials through fermentation of raw materials, such as rice wine/beer, rice cakes, and fish by producing organic acids to control putrefactive microorganisms and pathogens growth (Rhee *et al.*, 2011).

Lactic acid bacteria are commonly used in the fermentation of matrices containing a large amount of starch. Starch wastes are increasingly used for the production of lactic acid (Reddy *et al.*, 2008; Martinez *et al.*, 2013). It has been shown that sourdough fermentation improves the quality of maize-based bread by making the dough more cohesive, soft and less elastic through modifications of the starch granule properties (Falade *et al.*, 2014). Thus, the starch properties modification of the starch properties by LAF plays an important role on the improvement of the functional attributes of traditional cereal foodstuffs (Omar *et al.*, 2000; Diaz-Ruiz *et al.*, 2003; Rhee *et al.*, 2011). It has been also shown that sourdough fermentation reduces the glycemic response to bread (Scazzina *et al.*, 2009). Despite the extended uses of LAF in traditional and industrial processing of food matrices containing large amounts of starch (e.g., cereals and fruits), detailed analyses of the transformations undergone by starch granules are scant. Velikova *et al.* (2016) found evidence that amylolytic acid bacteria contain a basic pool of chromosomal genes for starch hydrolysis. In this scenario, glycogen synthesis and starch degradation occur in parallel. Alonso-Gomez *et al.* (2016) studied the physicochemical changes that take place in the fermentation of cassava for steeping times ranging

from 15 to 90 days at room temperature. Sour samples were collected from a local Colombian factory. The inoculums contained a large and uncontrolled diversity of lactic acid bacteria, including *Bifidobacterium inimum*, *Lactococcus lactis*, *Streptococcus* sp., *Enterococcus saccharolyticus* and *Lactobacillus plantarum*, *Lb. panis*, *Leuconostoc mesenteroides* and *Ln. citreum*. It was found that the acidification process produced significant structural changes in amylose and amylopectin as a function of the steeping time. Parada and Aguilera (2011) stated that several starch and food microstructures are responsible for the change in starch bioaccessibility, and that it is crucial to understand the role of the food matrix in relation to the metabolic effects.

Thus, the aim of this work was to characterize physicochemical transformations undergone by corn starch granules during lactic acid fermentation by *Lactobacillus bulgaricus*.

## 2 Materials and methods

---

### 2.1 Materials

Homofermentative *Lactobacillus delbrueckii subsp. Bulgaricus* (*L. bulgaricus* in short, ATCC® 11842<sup>TM</sup>), a strain producing mainly L-(+)-lactic acid, from the American Type Culture Collection was used in this work. Cultures were maintained at 4°C on slants containing 3% glucose along with the other essential nutrients. Lactic acid bacteria were revived by two successive propagations at 45°C for 12-18 h in the modified MRS broth, under anaerobic conditions. Native corn starch (NCS; S-4126, amylose content of 25.03 ± 0.62 g 100 g<sup>-1</sup>) was purchased from Sigma-Aldrich (St. Louis, MO, USA). Deionized water was used in all experiments.

### 2.2 Inoculum preparation

For inoculum preparation, 1 g of *L. bulgaricus* culture was dispersed in 10 mL of MRS medium (55 g L<sup>-1</sup>). The medium was incubated under anaerobic conditions in a MaxQ 7000 water bath orbital shaker (Terra Universal, Fullerton, CA, USA), at 38 °C and 200 rpm overnight, yielding 1 × 10<sup>7</sup> cells mL<sup>-1</sup>. Aliquots from this culture were used to inoculate starch fermentation trials.

### 2.3 Fermentation conditions

Erlenmeyer flasks (250 mL) containing native corn starch (NCS; 3% w/w) dispersions were inoculated under anaerobic conditions with  $2 \times 10^7$  cells mL<sup>-1</sup> of the *L. bulgaricus* culture. The flasks were gently stirred in the water bath orbital shaker at 38 °C, 200 rpm for up to 24 h. Fermented corn starch (FCS<sub>t</sub>, where the subindex t denotes the fermentation time) samples were withdrawn at different times, and centrifuged (6,000g) for 10 min. The precipitates were oven-dried at 30 °C until constant weight was achieved (~ 24 h), put into desiccators with a silica-gel bed at the bottom as desiccant, until required for analysis.

### 2.4 Polarized light microscopy and droplet size

Polarized light microscopy was used to examine the morphology of the FCS<sub>t</sub>. Samples were placed on viewing slides, upon which cover slips were gently placed. An Olympus BX45 microscope (Olympus Optical Co., Ltd., Tokyo, Japan) was used and images were captured with Carl Zeiss AxioCam ERc 5s camera (Hernández-Jaimes *et al.*, 2016). The mean number-length diameter ( $d_{1,0}$ ) of the NCS and FCSt was estimated by image analysis of the dispersions micrographs by means of the Zen-2012 software package (Carl Zeiss Microscopy GmbH). Selected micrographs at 100× are shown.

### 2.5 Scanning electron microscopy (SEM)

A JSM-7600F model scanning electron microscope (Jeol Co. Ltd., Tokyo, Japan) with the LM mode at 15 kV accelerating voltage was used to explore the microstructure of native and fermented starch granules. The dried samples were mounted on carbon sample holders using double-side sticky tape and sputtered with about 20 nm of gold using a Denton Vacuum DESK IV device. Selected micrographs at 500× are shown.

### 2.6 Amylose determination

Apparent amylose content of native and fermented starch dispersions was estimated by means of the iodine reagent method. To this end, 10 ml of KOH 0.5 M solution were added to 20 mg dry basis of starch sample and the suspension was mixed by vortex, and transferred to a 100 mL volumetric flask. Then, 5 ml of HCl 1.0 M solution was added, followed by 0.5 mL of the iodine reagent. The solution was diluted to 100

mL and the absorbance was measured at 620 nm on a Spectronics Genesys 5 UV/Vis spectrophotometer (Spectronic Unicam, Rochester, NY, USA) after 20 min. The apparent amylose determination of apparent amylose was carried out following a standard curve obtained by using different ratios of amylose and amylopectin mixtures.

### 2.7 X-ray diffraction (XRD)

A Bruker-AXS Model D8 Advance diffractometer (Bruker AXS GmbH, Karlsruhe, Germany) coupled to an X-ray diffraction copper anode tube was used to obtain the X-ray diffraction patterns of fermented starch granules, which were recorded with a scintillation counter. A nickel filter selected the CuK $\alpha$  radiation ( $\lambda = 1.543 \text{ \AA}$ ) and a secondary beam graphite monochromator was operated at 35 kV and 25 mA. Intensities were measured in the 10-30° diffraction angle range with a 0.03° step size and measuring time of 0.6 s per point.

### 2.8 Fourier transform infrared spectroscopy (FTIR)

The infrared spectra of fermented starch granules were recorded on a FTIR spectrophotometer (PerkinElmer FT-IR Spectrometer Frontier, Waltman, MA, USA). The samples were then subjected to attenuated total reflectance (ATR) spectroscopy in the range of 1200-900 cm<sup>-1</sup> (García-Dávila *et al.*, 2017).

### 2.9 Thermal characterization

The thermal properties of NCS and FCSt were analyzed by differential scanning calorimetry (DSC) (TA Instruments, Q1000, New Castle, DE, USA) previously calibrated with indium. Samples (2.5 mg of starch and 25.0 mg of water) were hermetically closed in aluminum pans and heated in a calorimeter from 25 to 150 °C at constant rate of 10 °C/min. An empty aluminum pan was used as reference. Temperatures ( $T_o$ - onset,  $T_p$  - peak,  $T_c$  - conclusion) and enthalpy change of thermal transitions ( $\Delta H$ , J g<sup>-1</sup> on dry basis) were determined with the use of the instrument's software Universal Analysis 2000 (TA Instruments, New Castle, DE, USA).

### 2.10 Viscosity of gelatinized dispersions

Gelatinized dispersions were prepared by dispersing the 5% w/w of dried fermented starch in deionized

water. The dispersions were gently stirred and heated at 90 °C for 20 min to allow complete gelatinization of the starch granules. Gelatinized dispersions were then cooled down to room temperature. The apparent viscosity was determined with a dynamic oscillatory Kinexus Pro rheometer (Malvern Instruments, Ltd., Worcestershire, UK), coupled to cone-plate geometry with a gap of 0.15 mm, in which the rotating cone was 40 mm in diameter and 4° in cone angle. About 1.6 mL of sample were carefully placed in the measuring system, and left to rest for 10 min at 25 °C for structure recovery and temperature equilibration. Flow curves of the gelatinized dispersions were determined by applying an increasing shear rate from 0.1 to 100 s<sup>-1</sup> and the apparent viscosity at a shear rate of 1 s<sup>-1</sup> is reported.

### 2.11 $\zeta$ -potential

The  $\zeta$ -potential of native and fermented starch dispersions (1% w/w) in deionized water was measured with a Zetasizer-Nano ZS (Malvern, Malvern Instruments Ltd., Malvern, Worcestershire, UK). All measurements were conducted at 20 °C. The instrument was calibrated by measuring the  $\zeta$ -potential of a standard sample, having  $\zeta$ -potential = -20±1 mV.

### 2.12 Acidic hydrolysis

The NCS and the FCSt granules (15 g, dry basis) were dispersed by stirring in an aqueous hydrochloric acid solution (100 mL, 1M), and kept at 38 °C. After 2 h, the reaction was stopped by neutralization (NaOH, 0.1 M) and centrifuging at 6,000g for 10 min for recovering non-hydrolyzed material. The precipitates were washed in deionized water until neutral pH was reached, air-dried at 35 °C for 24 h, and stored in a sealed glass container at 4 °C. The hydrolysis conversion was computed as the percent of precipitated and dried solids relative to the initial starch solids.

### 2.13 Statistical analysis

Statistical analysis of the results was performed using SAS software 9.3 (SAS Institute, Inc., Cary, NC, USA). One-way analysis of variance (ANOVA) ( $p < 0.05$ ) was performed.

## 3 Results and discussion

### 3.1 Results

Fig. 1.a presents the growth curve of the *L. bulgaricus* in MRS medium after 24 h of incubation. The growth

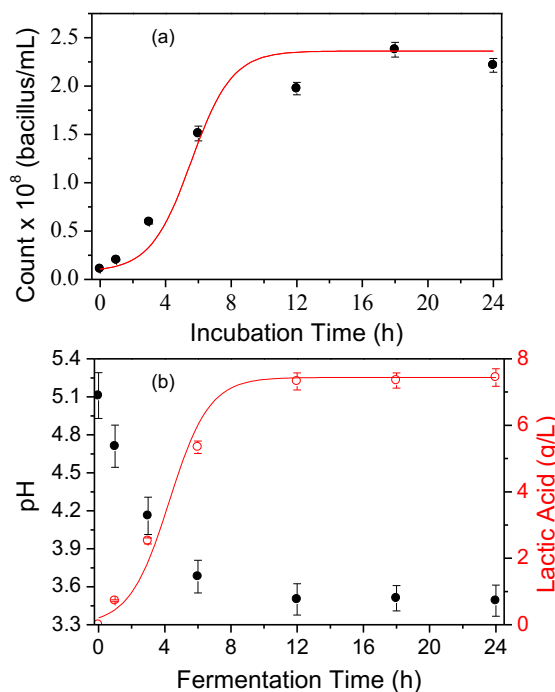


Fig. 1. (a) Growth kinetics of *L. bulgaricus* in MRS medium. (b) Evolution of the pH and lactic acid concentration with the fermentation time.

kinetics exhibited S-shaped pattern with lag time of about 2 h. The maximum cell population was about  $2.5 \times 10^8$  counts mL<sup>-1</sup>. Lactobacilli were harvested in the late log phase and used for inoculating the corn starch dispersions (3% w/w). It is noted that the log phase was achieved after about 10-12 h of fermentation time, suggesting that LAF should be conducted for at least this time period.

On the other hand, Fig. 1.b presents the pH variation with the fermentation time. Starting at ~5.1, the pH behavior showed an exponential-like decrease to achieve a steady value of ~3.4 after 12 h of fermentation time. This behavior concurs with the growth kinetics in Fig. 1.a where the growth plateau was achieved at about 10-12 h. The pH decrease was caused by the production of lactic acid, which is the main product of the fermentation of *L. bulgaricus*. Fig. 1.b also exhibits the kinetics of the lactic acid

concentration, which presented S-shaped pattern with a small lag phase of about 1 h. It is noted that the production of lactic acid was aligned with the decrease of the pH. The presence of the lactic acid in the fermentation medium should have an important effect in the transformations of the starch granules.

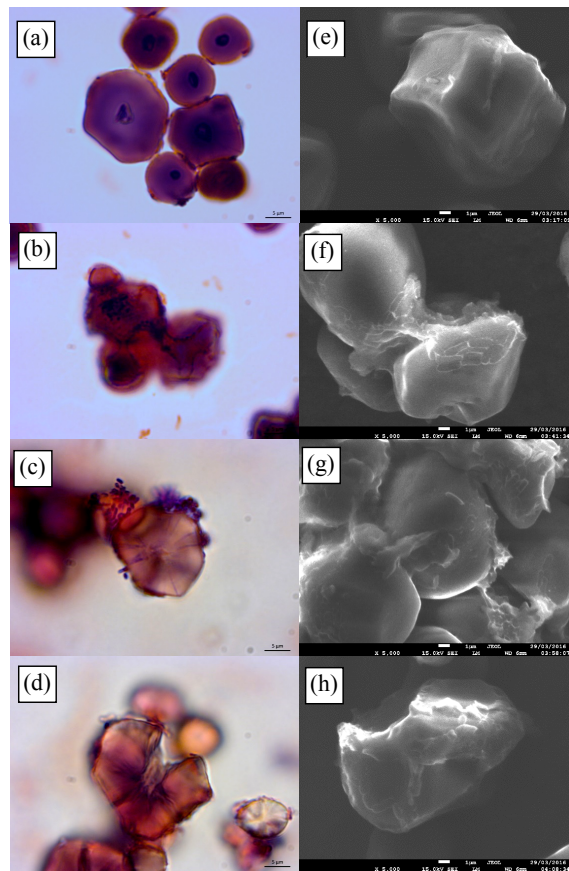


Fig. 2. (a)-(d) Light microscopy and (e)-(h) SEM images of native and fermented corn starch granules with *L. bulgaricus*.

In fact, lactic acid can undergo weak hydrolysis of carbohydrate polymeric chains at the operating fermentation temperature. For instance, it has been shown that lactic acid can hydrolyze chitosan chains under mild conditions (Il'Ina and Varlamov, 2004).

The morphology of fermented starch granules was explored with light and scanning electron microscopy. Fig. 2.a presents a light microscopy image of iodine-stained NCS granules freshly inoculated with *L. bulgaricus*. Granules showed the typical polygonal form with the hilum at the center of the granule. It is noted that the granule surface exhibited lactobacilli attachment, which was likely mediated by hydrogen binding (Imam and Harry-O'Kuru 1991). Figs.

2.b to 2.d illustrate the progressive morphological transformations undergone by the starch granules as fermentation time elapsed. After 3 h, just after the lag phase (Fig. 2.b), an increasing population of lactobacilli appeared surrounding the starch granules. Fig. 2.c shows that after 6 h a large number of lactobacilli invaded the hilum of a starch granule. The hilum, an organization center linked to the Malta cross, is a fragile outer point connecting with the internal granule structure. The attachment of lactobacilli to the hilum region marks the beginning of the granule structure breakdown via the action of the amylolytic enzymes produced by the lactobacilli. Figure 2.d illustrates the breakdown of starch granules after 18 h of fermentation time. Fractures appear around the Malta cross, whose definition commences to blur, and erosion at the granule circumference is noticed.

SEM images detailed the morphological changes induced by lactobacilli fermentation on the corn starch granules. Fig. 2.e illustrates the morphology (500 $\times$ ) of the NCS granule, showing a smooth surface not affected by enzymatic or lactic acid degradation. After 3 h, the fermented granules appeared as deflated balloons (Fig. 2.f) and after 6 h some fractures can be appreciated (Fig. 2.g). The integrity of the starch granules was further disrupted after 18 h of fermentation (Fig. 2.h), with severe erosion and fractures taking place. In turn, this led to the formation of a porous network in the vicinity of the hilum region (Fig. 2.d). An exfoliated appearance of the granule surface was noticed, probably induced by the combined action of the lactic acid and amylolytic enzymes produced by the lactobacilli population.

SEM images in Fig. 1 showed that the fermentative action led to important changes of the starch granules size as fractures and surface erosion reduced the mean size. This effect was evaluated by monitoring of the mean number-length diameter (i.e., linear diameter) and the results are presented in the first column of Table 1. As expected,  $d_{1,0}$  decreased with the fermentation time, which is a direct consequence of surface erosion and granule fragmentation induced by the activity of amylolytic enzymes. It is also noted that the reduction of the granule size was accompanied by increasingly large standard deviations, which in turn reflects a diversity of granular structures formation.

Table 1 presents the changes of the amylose/amylopectin ratio with the fermentation time. The relative content of amylose decreased during the first 6 h. Linear amylose chains are more susceptible to enzymatic hydrolysis than branched amylopectin chains, leading to the reduction of the amylose content

at short fermentation times. However, the ratio showed a slight increase at longer fermentation times. This effect can be linked to short chains debranched from

amylopectin, which are detected as apparent amylose chains (Naguleswaran *et al.*, 2014).

Table 1. Evolution of physicochemical parameters with the fermentation time.

Fermentation time (h)	$d_{1,0}$ ( $\mu\text{m}$ )	Amylose/ Amylopectine Ratio	Crystallinity (%)	Absorbance Ratio 1047/1022	$\zeta$ -Potential (mV)	Viscosity at 1.0 s <sup>-1</sup> (Pa · s)	Two-hours HCl hydrolysis (%)
<b>Native</b>	17.31±0.67a	0.37±0.01a	32.88±2.12c	0.64±0.03a	-	8.48±0.34a	36.96±1.43a
<b>1</b>	16.28±0.76ab	0.34±0.02b	33.73±1.24c	0.64±0.02a	15.12±0.67d	6.83±0.27b	28.78±1.65b
<b>3</b>	13.35±0.78b	0.32±0.02bc	37.44±1.13ab	0.65±0.03a	21.43±0.75c	4.40±0.35c	25.83±1.73c
<b>6</b>	10.74±0.96c	0.32±0.02bc	39.72±1.02a	0.67±0.03ab	23.71±0.83b	3.50±0.24cd	19.18±1.42d
<b>12</b>	7.08±1.9d	0.33±0.02bc	38.84±0.95a	0.72±0.04c	25.27±0.81ab	2.98±0.14d	15.98±1.59e
<b>24</b>	6.07±1.13d	0.36±0.02a	37.32±0.96ab	0.78±0.03d	30.25±0.91a	2.64±0.17de	9.37±1.21f
					28.68±0.96a		

aMeans (± standard deviation) in a column followed by different letters are significantly different ( $p \leq 0.05$ ).

Table 1 also presents the  $\zeta$ -potential values. NCS displayed negative  $\zeta$ -potential of relatively small magnitude (about -14.21 mV). The NCS added with *L. bulgaricus* displayed a  $\zeta$ -potential magnitude of about -15.12 mV. A gradual increase of the  $\zeta$ -potential magnitude occurred with the advance of the fermentation time, being of about -26.68 mV after 24 h. Amyolytic enzymes fragmented starch chains to ultimately yield glucose. The lactic acid bacteria metabolize this substrate producing alcohol, pyruvate and lactate, among other intermediate products (Reddy *et al.*, 2008). The observed increase of the  $\zeta$ -potential magnitude (in the negative domain) might be explained from the proliferation of these products expressing negative potential values (e.g., ethanol). In this way, the evolution of the  $\zeta$ -potential reflects the advance of the starch chain hydrolysis by the metabolic action of the lactobacilli.

The results of acid hydrolysis are presented in the last column of Table 1. The NCS granules were hydrolyzed up to 37.12%. FCS<sub>t</sub> granules were less prone to acidic hydrolysis the longer was the fermentation time to which they were subjected. The FCS<sub>24</sub> exhibited only a 9.37% hydrolysis. The decline in the acidic hydrolysis advance with fermentation time can be linked to the increase of the crystallinity content. In fact, well-ordered crystalline structures are less susceptible of hydrolysis by acidic and

enzymatic digestion. It has been reported that rice starch incubated with amyolytic enzymes changed the digestibility properties by decreasing the fraction of rapidly digestible starch at the expenses of increasing the fraction of slowly digestible starch (Zhang *et al.*,

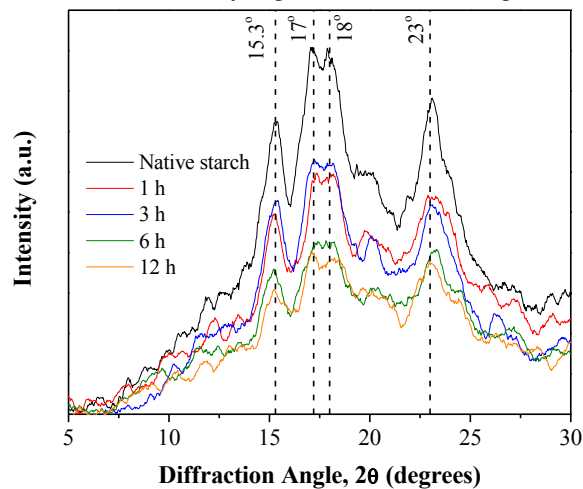


Fig. 3. X-ray diffraction patterns for native and fermented corn starch with *L. bulgaricus*. Vertical lines denote distinctive peaks of Type-A crystallinity.

2016).

Fig. 3 presents the X-ray diffractions patterns of native and fermented starch granules. NCS presented

the typical A-type XRD pattern, with main intensity peaks at 15.12, 17.17, 18.05 and 23.0  $2\theta$ -degrees (Buléon, *et al.*, 1998). The FCS<sub>t</sub> granules also presented this crystallinity pattern, suggesting that the starch crystalline structure was not altered by the fermentative action of the lactobacilli population. The crystallinity content of the native and fermented starch granules is presented in the second column of Table 1. The crystallinity of the NCS was about 32.82%. In the first 12 h, the crystallinity content

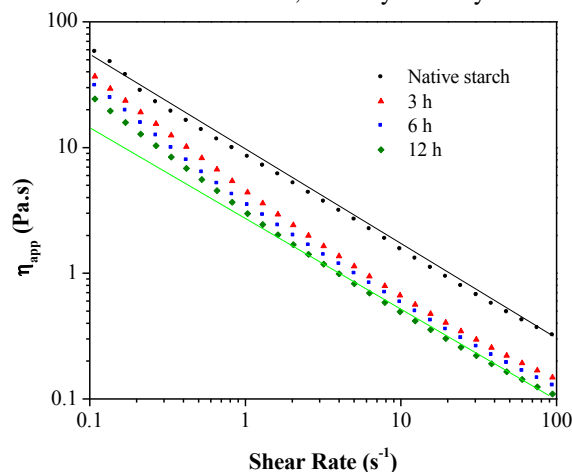


Fig. 4. Apparent viscosity as function of the shear rate for native and corn starch fermented with *L. bulgaricus*.

increased to maximum value of about 39.72%. At longer fermentation times the crystallinity content exhibited a slight decrease. A similar effect was observed for hydrolysis with sulfuric acid (Utrilla-Coello *et al.*, 2014), suggesting that the initial increase in crystallinity was linked to the preferred attack of the amorphous regions of the starch granules by the amylolytic enzymes produced by the lactobacilli population.

The absorbance bands at 1047 and 1022  $\text{cm}^{-1}$  linked respectively to crystalline and amorphous structures of starch were explored.

The absorbance ratio 1047  $\text{cm}^{-1}$ /1022  $\text{cm}^{-1}$  is commonly taken as an index of the ordered crystalline domains to amorphous domains in starch (van Soest *et al.*, 1995). The third column in Table 1 shows the absorbance ratio 1047  $\text{cm}^{-1}$ /1022  $\text{cm}^{-1}$  as function of the fermentation time. The absorbance ratio remained nearly unaltered during the first 12 h, showing a decrease at longer times. This result is in line with the crystallinity content estimated from the XRD pattern.

Fig. 4 presents the apparent viscosity pattern of

starch pastes (5% w/w) as function of the shear rate. The apparent viscosity pattern was described by a power-law function of the form  $\eta_{app} = K_n \dot{\gamma}^{n-1}$ , where  $\dot{\gamma}$  is the shear-rate,  $K_n$  is the flow consistency index, and  $n$  is the flow behavior index ( $n < 1$  for shear-thinning fluids). For NCS,  $n = 0.72 \pm 0.02$  with  $R^2 = 0.93$ . The same value adjusted the experimental data for the fermented granules, but only for shear rate values higher than 1.0  $\text{s}^{-1}$ . For smaller shear rate values,  $n = 0.95 \pm 0.02$  with  $R^2 = 0.96$ , which reflects a near Newtonian-like behavior.

Table 2 presents the thermal properties of the hydrolyzed starch granules as estimated by DSC measurements. The melting temperature range  $T_c - T_o$  increased with the fermentation time, reflecting that fermented starch granules exhibited a more heterogeneous structure than the NCS granules. The gelatinization enthalpy also increased with the fermentation time, which is related to more ordered microstructures induced by the fermentation process. The slight decrease showed after 12 h might be related to the long-term deterioration of the crystallinity as detected by the XRD measurements. Interestingly, similar results were found by Utrilla-Coello *et al.* (2014), reporting that parabolic relationship between gelatinization enthalpy and relative crystallinity for corn starch hydrolyzed with  $\text{H}_2\text{SO}_4$  (3.6 M, 35 °C).

### 3.2 Discussion

The fermentative action of *Lactobacillus bulgaricus* induced important changes in morphology and physicochemical characteristics of corn starch granules. Surface erosion and fractures along the hilum showed to be the dominant mechanism involved in morphological changes. Amylolytic enzymes (mainly,  $\alpha$ -amylase) produced by the attached lactobacilli eroded the outer region around the Malta Cross to penetrate the internal structure via the hilum. Then, the breakdown of the granule became a consequence of the degradation of the inner most amorphous starch chains rings. Native starch granules are formed by radially oriented semi-crystalline regions and amorphous growth rings organized about the hilum.

The starch granule is a stable structure and the hilum region appears as disorganized with some fractures. Images in Fig. 2 reflected that the granule disruption by the fermentative action of the bacillus started around the hilum fractures. After an adaptation period during the lag phase, the lactobacilli population grew and was able to produce amylolytic enzymes

that attacked the vulnerable region located around the Malta cross. Although the granule surface was also eroded by the amylolytic activity, the amorphous growth regions within the granule structure are more susceptible to degradation by amylolytic enzymes. The fracture passing through the hilum allowed the

diffusion of lactic acid and amylolytic enzymes (Chen *et al.*, 2006). Eventually, after about 12 h, the starch granules were cracked down, leaving an amorphous and largely disrupted structure. The fermentative action of *L. bulgaricus* is slower than the action by the direct application of amylolytic enzymes.

Table 2. Evolution of the thermal properties of fermented corn starch at different times with *L. bulgaricus*.

Fermentation Time (h)	Onset Temperature $T_o$ (°C)	Peak Temperature $T_p$ (°C)	Conclusion Temperature $T_c$ (°C)	Temperature Range $T_c - T_o$ (°C)	Enthalpy Change $\Delta H$ (J/g)
Native	57.65±0.32a	72.16±0.26a	86.13±0.92a	27.91±0.25	7.65±0.31a
1	57.22±0.54a	71.54±0.25b	86.71±0.35a	29.49±1.17	7.76±0.32a
3	55.36±0.23b	72.62±0.12a,b	85.25±0.54b	29.89±0.57	9.69±0.68b
6	55.98±0.78a,b	73.29±0.38c	88.67±0.89c	32.69±1.16	11.19±0.28a,b
12	54.14±0.47b	74.54±0.42c	89.09±0.25c	34.95±0.76	10.13±0.47c
24	56.54±0.43a	74.72±0.61c	92.13±0.51d	35.59±0.86	9.93±0.72d

<sup>a</sup>Means (± standard deviation) in a column followed by different letters are significantly different ( $p \leq 0.05$ ).

In fact, the direct activity of added amylase is much faster, taking about 8 hours to achieve 90% of starch hydrolysis (Shresta *et al.*, 2012, 2015). It has been pointed out that diffusion-controlled superficial and porous erosions are the dominant mechanisms involved in the degradation of starch granules by amylolytic (e.g., amylase) activity (Shrestha *et al.*, 2012). It is noted that the reduction of the granule size was accompanied by increasingly large standard deviations, which in turn reflects a diversity of granular structures formation.

Although  $\alpha$ -amylase attacks both the crystalline and amorphous regions, the latter region is more susceptible to amylolytic digestion than the former (Shresta *et al.*, 2012). Besides, the formation of pores and channels enhances the physical penetrability of the enzymes into the amorphous regions of the starch granules. The combined effect of the enzymatic and acidic hydrolysis enlarged the porous network of the granule (see Figs. 2.c and 2.d), leading to an increased rate of starch chain fragmentation. Zhang *et al.* (2016) reported similar results for treated starch with  $\alpha$ -amylase and amyloglucosidase, where the crystallinity showed a slight increase during the initial hydrolysis period. Similarly, Li *et al.* (2013) found that amylolytic enzymes obtained from rice leaven increased the crystallinity of rice starch under mild conditions.

On the other hand, the FTIR results in Table 1 suggested that in the first 12 h period, the amylolytic enzymes produced by the lactobacilli population

hydrolyzed the amorphous regions of the starch granules while leaving untouched the double-helices arrangements. In the midpoint of the fermentation period, the long-range crystallinity achieved a maximum value as the amount of amorphous regions was reduced. The gradual disruption of the granule structure at long fermentation times exposed the crystalline regions to the combined action of the amylolytic enzymes and the lactic acid, producing the reduction of the crystallinity percentage. In this process, the double-helices content was positively affected, leading to an increase of the short-range crystallinity content.

The reduction of the apparent viscosity with the fermentation time can be explained as follows. Amylose and amylopectin chains are leached out from starch granules during the gelatinization process, producing a highly viscous continuous matrix. Insoluble remnants, also called ghosts, are dispersed in the continuous matrix to form a microstructure with complex viscoelastic response (Debet and Gidley 2007). The chain length and ramifications degree of leached starch chains have strong influence on the viscoelastic properties. Specifically, the stability of the 3D viscous network is largely determined by linear amylose chains (Zhang *et al.*, 2013). The reduction of the apparent viscosity with the fermentation advance suggests that the enzymatic hydrolysis coupled to the lactic acid hydrolysis, affected primarily the amylose molecules, which on turn led to fragile microstructure networks (i.e., weaker gels) with reduced viscosity.

Eventually, the amylose content was drastically reduced and the branched amylopectin molecules dispersed in the continuous network and attached to the insoluble remnants were also hydrolyzed.

Finally, the reduction of the susceptibility to acid hydrolysis with the fermentation time is interesting. The side-by-side digestion mechanism (Zhang and Hamaker 2009) postulates that granules of A-type starches contain channels connecting the central region to the granule surface, facilitating the penetration of enzymes and acid molecules. These channels are consequence of amorphous arrangements, which are firstly degraded by hydrolysis reactions. In this way, the reduced acidic hydrolysis of starch would be the consequence of granules fragments with increased crystallinity and reduced porosity. From a kinetics viewpoint, the acidic hydrolysis is limited by the transport of protons into the starch structure.

## Conclusions

---

Lactic acid fermentation with *L. bulgaricus* induced large changes in the morphology of corn starch granules. The production of amylolytic enzymes as well as lactic acid produced fractures along the granule hilum, which led to disintegration of starch granules at long fermentation times. On the other hand, lactic acid fermentation increased crystallinity and double-helices structures, which led to increased susceptibility to acidic hydrolysis. In fact, thermal analysis results indicated than an improved internal organization of granule residues occurred. In general, the results showed that the fermentation time can be considered as a suitable parameter for modulating the physicochemical properties of corn starch granules. Additionally, it can be postulated that lactic acid fermentation of starchy food matrices has a positive effect on the acidic digestibility of starch granules, by improving the content of resistant starch fractions.

## References

---

Abdel-Rahman, M. A., Tashiro, Y., and Sonomoto, K. (2013). Recent advances in lactic acid production by microbial fermentation processes. *Biotechnology Advances* 31, 877-902.

Alonso-Gomez, L., Niño-López, A. M., Romero-Garzón, A. M., Pineda-Gomez, P., del Real-Lopez, A., and Rodriguez-Garcia, M. E. (2016). Physicochemical transformation of cassava starch during fermentation for production of sour starch in Colombia. *Starch/Stärke* 68, 1139-1147.

Buléon, A., Colonna, P., Planchot, V., and Ball, S. (1998). Starch granules: Structure and biosynthesis. *International Journal of Biological Macromolecules* 23, 85-112.

Chen, P., Yu, L., Chen, L., and Li, X. (2006). Morphology and microstructure of maize starches with different amylose/amylopectin content. *Starch/Stärke* 58, 611-615.

Datta, R., and Henry, M. (2006). Lactic acid: recent advances in products, processes and technologies-A review. *Journal Chemical Technology Biotechnology* 81, 1119-1129.

Debet, M. R., and Gidley, M. J. (2007). Why do gelatinized starch granules not dissolve completely? Roles for amylose, protein, and lipid in granule "ghost" integrity. *Journal of Agricultural and Food Chemistry* 55, 4752-4760.

Di Cagno, R., Coda, R., De Angelis, M., and Gobbetti, M. (2013). Exploitation of vegetables and fruits through lactic acid fermentation. *Food Microbiology* 33, 1-10.

Diaz-Ruiz, G., Guyot, J. P., Ruiz-Teran, F., Morlon-Guyot, J., and Wachter, C. (2003). Microbial and physiological characterization of weakly amylolytic but fast-growing lactic acid bacteria: a functional role in supporting microbial diversity in pozol, a Mexican fermented maize beverage. *Applied and Environmental Microbiology* 69, 4367-4374.

Falade, A. T., Emmambux, M. N., Buys, E. M., and Taylor, J. R. (2014). Improvement of maize bread quality through modification of dough rheological properties by lactic acid bacteria fermentation. *Journal of Cereal Science* 60, 471-476.

García-Dávila, J., Ocaranza-Sánchez, E., Sánchez, C., Ortega-Sánchez, E., Tecluitl-Beristaín, S., and Martínez-Ayala, A. L. (2017). FTIR analysis of hydrotreated *Jatropha curcas* L. seed

- oil over Ni-Mo catalyst for biofuel production. *Revista Mexicana de Ingeniería Química* 16, 337-345.
- Hernández-Jaimes, C., Meraz, M., Lara, V. H., González-Blanco, G., and Buendía-González, L. (2017). Acid hydrolysis of composites based on corn starch and trimethyleneglycol as plasticizer. *Revista Mexicana de Ingeniería Química* 16, 169-178.
- Il'Ina, A. V., and Varlamov, V. P. (2004). Hydrolysis of chitosan in lactic acid. *Applied Biochemistry Microbiology* 40, 300-303.
- Imam, S. H., and Harry-O'Kuru, R. E. (1991). Adhesion of *Lactobacillus amylovorus* to insoluble and derivatized cornstarch granules. *Applied and Environmental Microbiology* 57, 1128-1133.
- Leroy, F., and De Vuyst, L. (2004). Lactic acid bacteria as functional starter cultures for the food fermentation industry. *Trends in Food Science & Technology* 15, 67-78.
- Li, H., Jiao, A., Wei, B., Wang, Y., Wu, C., Jin, Z., and Tian, Y. (2013). Porous starch extracted from Chinese rice wine vinasse: Characterization and adsorption properties. *International Journal Biological Macromolecules* 61, 56-159.
- Martinez, F. A. C., Balciunas, E. M., Salgado, J. M., González, J. M. D., Converti, A., and de Souza Oliveira, R. P. (2013). Lactic acid properties, applications and production: a review. *Trends in Food Science & Technology* 30, 70-83.
- Naguleswaran, S., Vasanthan, T., Hoover, R., and Bressler, D. (2014). Amylolysis of amylopectin and amylose isolated from wheat, triticale, corn and barley starches. *Food Hydrocolloids* 35, 686-693.
- Omar, N. B., Ampe, F., Raimbault, M., Guyot, J. P., and Tailliez, P. (2000). Molecular diversity of lactic acid bacteria from cassava sour starch (Colombia). *Systematic Applied Microbiology* 23, 285-291.
- Parada, J., and Aguilera, J. M. (2011). Review: starch matrices and the glycemic response. *Food Science and Technology International* 17, 187-204.
- Reddy, G., Altaf, M. D., Naveena, B. J., Venkateshwar, M., and Kumar, E. V. (2008). Amylolytic bacterial lactic acid fermentation-a review. *Biotechnology Advances* 26, 22-34.
- Rhee, S. J., Lee, J. E., and Lee, C. H. (2011). Importance of lactic acid bacteria in Asian fermented foods. *Microbial Cell Factories* 10, S5.
- Scazzina, F., Del Rio, D., Pellegrini, N., and Brighenti, F. (2009). Sourdough bread: Starch digestibility and postprandial glycemic response. *Journal of Cereal Science* 49, 419-421.
- Shiby, V. K., and Mishra, H. N. (2013). Fermented milks and milk products as functional foods-A review. *Critical Reviews in Food Science and Nutrition* 53, 482-496.
- Shrestha, A. K., Blazek, J., Flanagan, B.M., Dhital, S., Larroque, O., Morell, M. K., and Gidley, M. J. (2012). Molecular, mesoscopic and microscopic structure evolution during amylase digestion of maize starch granules. *Carbohydrate Polymers* 90, 23-33.
- Shrestha, A. K., Blazek, J., Flanagan, B. M., Dhital, S., Larroque, O., Morell, M. K., and Gidley, M. J. (2015). Molecular, mesoscopic and microscopic structure evolution during amylase digestion of extruded maize and high amylose maize starches. *Carbohydrate Polymers* 118, 224-234.
- Utrilla-Coello, R.G., Hernández-Jaimes, C., Carrillo-Navas, H., González, F., Rodríguez, E., Bello-Perez, L. A., Vernon-Carter, E. J., and Alvarez-Ramirez, J. (2014). Acid hydrolysis of native corn starch: morphology, crystallinity, rheological and thermal properties. *Carbohydrate Polymers* 103, 596-602.
- van Soest, J. J., Tournois, H., de Wit, D., and Vliegenthart, J. F. (1995). Short-range structure in (partially) crystalline potato starch determined with attenuated total reflectance Fourier-transform IR spectroscopy. *Carbohydrate Research* 279, 201-214.
- Velikova, P., Stoyanov, A., Blagoeva, G., Popova, L., Petrov, K., Gotcheva, V., Angelov, A., and Petrova, P. (2016). Starch utilization routes in lactic acid bacteria: new insight by gene expression assay. *Starch/Stärke* 68, 953-960.

- Zhang, G., and Hamaker, B.R. (2009). Slowly digestible starch: concept, mechanism, and proposed extended glycemic index. *Critical Reviews in Food Science and Nutrition* 49, 852-867.
- Zhang, T., Li, X., Chen, L., and Situ, W. (2016). Digestibility and structural changes of waxy rice starch during the fermentation process for waxy rice vinasse. *Food Hydrocolloids* 57, 38-45.
- Zhang, C., Zhu, L., Shao, K., Gu, M., and Liu, Q. (2013). Toward underlying reasons for rice starches having low viscosity and high amylose: physiochemical and structural characteristics. *Journal of the Science of Food and Agriculture* 93, 1543-1551.